Applied Catalysis A: General 464–465 (2013) 142–148

Contents lists available at SciVerse ScienceDirect

Applied Catalysis A: General

journal homepage: www.elsevier.com/locate/apcata

Synthesis of dipropyl carbonate over calcined hydrotalcite-like compounds containing La

Qingxiang Ma[a,b], Tiansheng Zhao[b,*], Ding Wang[a], Wenqi Niu[a], Peng Lv[a], Noritatsu Tsubaki[a,**]

[a] Department of Applied Chemistry, School of Engineering, University of Toyama, Gofuku 3190, Toyama 930-8555, Japan
[b] State Key Laboratory Cultivation Base of Natural Gas Conversion, Ningxia University, Yinchuan 750021, China

ARTICLE INFO

Article history:
Received 22 March 2013
Received in revised form 13 May 2013
Accepted 19 May 2013
Available online 6 June 2013

Keywords:
Dipropyl carbonate
Transesterification
Hydrotalcite-like compounds
Composite oxide
DMC

ABSTRACT

Dipropyl carbonate (DPC) was selectively synthesized via transesterification of dimethyl carbonate (DMC) and n-propanol over Mg–Al composite oxide containing La catalysts. The catalysts were prepared by calcining the precursors of hydrotalcite-like compounds (HTLcs) from co-precipitation method. The effect of La content (n_{Mg}:n_{Al}:n_{La} = 3:1:x) in the catalyst on the synthesis of DPC was investigated. And the catalyst exhibited the highest catalytic activity when x was tuned to 0.7. Under the optimized reaction conditions, the DMC conversion and DPC selectivity were 98.4% and 95.4%, respectively. These catalysts were characterized by thermogravimetry differential thermal analysis (TG-DTA), X-ray diffraction (XRD), nitrogen adsorption–desorption, Fourier transform infrared (FT-IR), temperature programmed desorption with CO_2 (CO_2-TPD) and scanning electron micrograph (SEM). It was clarified that the amount of basic sites of moderate strength, formed by chelating bidentate carbonate, was enhanced with the La content increasing until x = 0.7, which were the catalytically-active sites for this reaction. But when La content x reached 1.0, these sites were transformed to bridging bidentate carbonate, leading to a loss of the catalytic activity to some extent. These findings indicated that La content controlled the catalytic performance of the composite oxides catalysts via structure change of the basic sites. The catalyst was easily prepared and handled, easily separated from the reaction medium and could be reused many cycles.

1. Introduction

Dipropyl carbonate (DPC), containing both propoxy and carbonyl groups, is an important synthesis intermediate as a useful propylating and propoxycarbonylating agent for synthesis of many organic compounds. It is also widely used as electrolyte in lithium ion batteries for its high dielectric constants [1]. Compared to dimethyl carbonate (DMC) and diethyl carbonate (DEC), DPC has larger molecular weight, higher flash point and stronger antioxidation than that of DMC and DEC, it can be used as a more stable and safer electrolyte for lithium ion batteries in extreme environment such as high temperature and oxygen environment [2].

Traditionally, DPC was synthesized by the reaction of phosgene or dimethylsulfate with propanol. But this synthesis method has many disadvantages such as reactant containing toxic phosgene, dimethylsulfate and generating the by-products hydrochloric acid. It would make serious corrosion of reaction equipment and environmental pollution. Meanwhile, the conversion of reactants is very low [3,4]. Therefore, a new approach of synthesis of DPC becomes more attractive to researchers. Recent years, DMC has been paid extensive attention as an important green chemical material which is nontoxic and easily biodegradable; it can be used as esterification and transesterification reagent instead of dimethylsulfate and phosgene in carbonylation process. Both symmetric and asymmetric organic carbonates can be synthesized via transesterification reactions using DMC as a raw material [5–12]. In general, transesterification reactions are carried out in the liquid phase using homogeneous catalysts such as bases, organic Mo, Sn or Ti compounds, and so on [13–16]. However, this process has an obvious disadvantage due to the difficulty of separation. Therefore, development of active solid catalysts is desirable. As far as we know, there are only few researches reported on the DPC synthesis by transesterification with DMC and n-propanol. Li et al. investigated the DPC synthesis from DMC and propanol catalyzed over KNO_3/MCM-48 by transesterification. Although the activity was high, the preparation of the catalysts was very complicated while mesoporous MCM-48 was not stable [17]. Chen et al. studied the synthesis of

* Corresponding author. Tel.: +86 951 206 2237; fax: +86 951 206 2237.
** Corresponding author. Tel.: +81 76 445 6846; fax: +81 76 445 6846.
E-mail addresses: zhaots@nxu.edu.cn (T. Zhao), tsubaki@eng.u-toyama.ac.jp (N. Tsubaki).

0926-860X/$ – see front matter © 2013 Elsevier B.V. All rights reserved.
http://dx.doi.org/10.1016/j.apcata.2013.05.026

methyl propyl carbonate (MPC) over supported TiO_2/Al_2O_3 via gas-phase transesterification [18], but DPC was the co-product with low selectivity in the process. In their reports, base sites were responsible for the catalytic activity during the transesterificati on reaction.

Hydrotalcite (HT) or hydrotalcite-like compounds (HTLcs) are layered double hydroxides belonging to anionic clays. The general formula of these compounds can be represented as:

$$[M(II)_{1-x}M(III)_x(OH)_2] \cdot A^{n-}_{x/n} \cdot mH_2O$$

Their layer structure is very similar to that of brucite, where part of Mg^{2+} cations or divalent cations represented as [M(II)] could be isomorphously substituted replaced by Al^{3+} or other trivalent metal cations represented as [M(III)], forming positively charged layers. The excess positive charge of brucite-like sheets is compensated by the inter-layer anions (A^{n-}) such as $CO_3{}^{2-}$ or OH^-. The advantage of this kind of HTLcs is that the basic properties can be easily controlled by the $M^{3+}/(M^{2+}+M^{3+})$ ratio, and the stoichiometric coefficient (x) may be assorted over a wide range ($0.25 < x < 0.44$) [19,20]. In addition, the thermal decomposition of these compounds at above 450 °C results in the formation of basic compound oxides with high surface areas, which show high catalytic activity in many reactions such as aldol condensation, Michael addition, transesterification and so on [21–26].

In this study, we prepared Mg–Al composite oxides containing La from hydrotalcite-like precursor via co-precipitation method. The physicochemical properties of the catalysts were studied by XRD, BET, TG-DTA, FT-IR, CO_2-TPD and SEM. The catalytic performance of catalysts for the DPC synthesis via the transesterification of DMC with propanol was investigated. The reaction can usually be completed via the following two steps:

$$CH_3OCOOCH_3 + C_3H_7OH \rightarrow C_3H_7OCOOCH_3 + CH_3OH \quad (1)$$

$$C_3H_7OCOOCH_3 + C_3H_7OH \rightarrow C_3H_7OCOOC_3H_7 + CH_3OH \quad (2)$$

2. Experimental

2.1. Catalyst preparation

Hydrotalcite-like samples of the catalyst were synthesized by the co-precipitation method. 0.03 mol (7.69 g) $Mg(NO_3)_2{\cdot}6H_2O$, 0.01 mol (3.75 g) $Al(NO_3)_3{\cdot}9H_2O$ and the fixed amount of $La(NO_3)_3{\cdot}H_2O$ (AR) were dissolved in deionized water of 400 mL at the molar ratios of Mg:Al:La = 3:1:0, 3:1:0.1, 3:1:0.4, 3:1:0.7, 3:1:1, respectively. Then an aqueous solution of Na_2CO_3 and NaOH (2:1, Na^+: 1.5 mol/L) was slowly dropped at a constant rate of 3 mL/min into the solution of nitrates under vigorous stirring until the pH value reached 10. The slurry was continuously stirred for 0.5 h and then kept at room temperature for 20 h. The slurry was then filtrated and washed with deionized water until the pH value reached 7.0. The resulting cake was dried at 80 °C for 10 h to obtain the HTLcs samples. Finally, the catalysts were calcined in air at 650 °C for 5 h with a heating rate of 10 °C/min. The obtained HTLcs samples and composite oxide catalysts were denoted as xLa-HTLcs before calcination and xLHTs after calcination, respectively, where x represented the added molar amount of La.

2.2. Catalyst characterization

Nitrogen adsorption measurements were carried out at −196 °C using a Quantachrome Instruments NOVA 2200e, while BET surface area and the pore size distribution were determined from the isotherms. The sample was out-gassed at 200 °C for 2 h before each test. Powder X-ray diffraction (XRD) patterns of the samples were measured at a Rigaku D/MAX2200PC X-ray differactometer using Cu Kα radiation. Thermogravimetric analysis (TGA) system was performed with DTG-60 instrument under air atmosphere (50 ml/min) with a heating rate of 10 °C/min from room temperature to 800 °C to estimate thermal decomposition behavior of catalyst. The basicity of catalysts was studied by the temperature programmed desorption (TPD) with CO_2. The TPD of CO_2 was carried out between 50 and 700 °C under a helium flow (30 ml/min) with a heating rate of 10 °C/min. Before the test, the samples were pretreated under helium atmosphere at 500 °C for 1 h, then, cooled to 50 °C, and exposed to pure CO_2 (30 ml/min) for 0.5 h. The Fourier transform infrared spectroscopy (FT-IR) spectra were recorded using the KBr pellet technique on a FT-IR spectrometer in the 4000–400 cm^{-1} range. SEM images were obtained at an amplifying time of 5000 on a JEOL JSM-6360LV instrument.

2.3. Catalytic activity tests

The catalytic activities of the composite oxides xLHTs for the DPC synthesis via transesterification were evaluated in a one-neck round bottom flask with a rotary evaporator. The freshly prepared powder catalysts were placed in the flask along with liquid reactant of DMC/n-propanol with an initials molar ratio of 1:3. The reaction was conducted at 90 ± 2 °C at an atmospheric pressure. The reaction time was 6 h. The dosage of the catalyst was defined as weight percentage of the reactants. The co-product of methanol was evaporated and separated from reaction system during the reaction.

The products were analyzed on a SP-2100 gas chromatography with a flame ionization detector (FID) and a separation column packed with polyglycol 20 M. The column was temperature-programmed from 100 °C to 150 °C.

3. Results and discussion

3.1. Catalyst characterization

3.1.1. TG-DTA analysis

The thermal decomposition behavior of La-HTLcs is studied. The TG-DTA curves of samples are shown in Fig. 1. The TG profile indicates two major weight losses at around 150 °C and 400 °C. The first weight loss is due to the elimination of physical adsorbed water and CO_2, interlayer water molecules, along with small amounts of weakly bound OH groups, and the weight loss is about 10%. This weight loss is associated with an endothermic peak around 200 °C with an endothermic shoulder peak around 85 °C, corresponding to the dehydroxylation of Al—OH and the physical adsorbed molecules, respectively [27]. The second weight loss is corresponded to dehydroxylation of samples. This weight loss is accompanied by an endothermic band for 0La-HTLcs and 0.1 La-HTLcs. This endothermic band is due to the dehydroxylation of Mg—OH. However, there are two endothermic bands for other samples. The first endothermic band belongs to dehydroxylation of Mg—OH and the second endothermic band is due to dehydroxylation of La—OH [28]. Above 700 °C, no obvious weight losses were observed, but very small exothermic peaks could be observed because the crystallization of new phase took place [29].

3.1.2. Nitrogen adsorption–desorption analysis

The N_2 adsorption–desorption isotherms were used to determine the pore structure of the catalysts. The N_2 adsorption–desorption isotherms and the corresponding pore size distribution of the xLHTs catalysts are shown in Fig. 2, respectively. All the samples exhibit typical type-IV adsorption isotherms with clear hysteresis loops at higher relative pressure, suggesting that mesopores appear in the samples. The hysteresis loops have

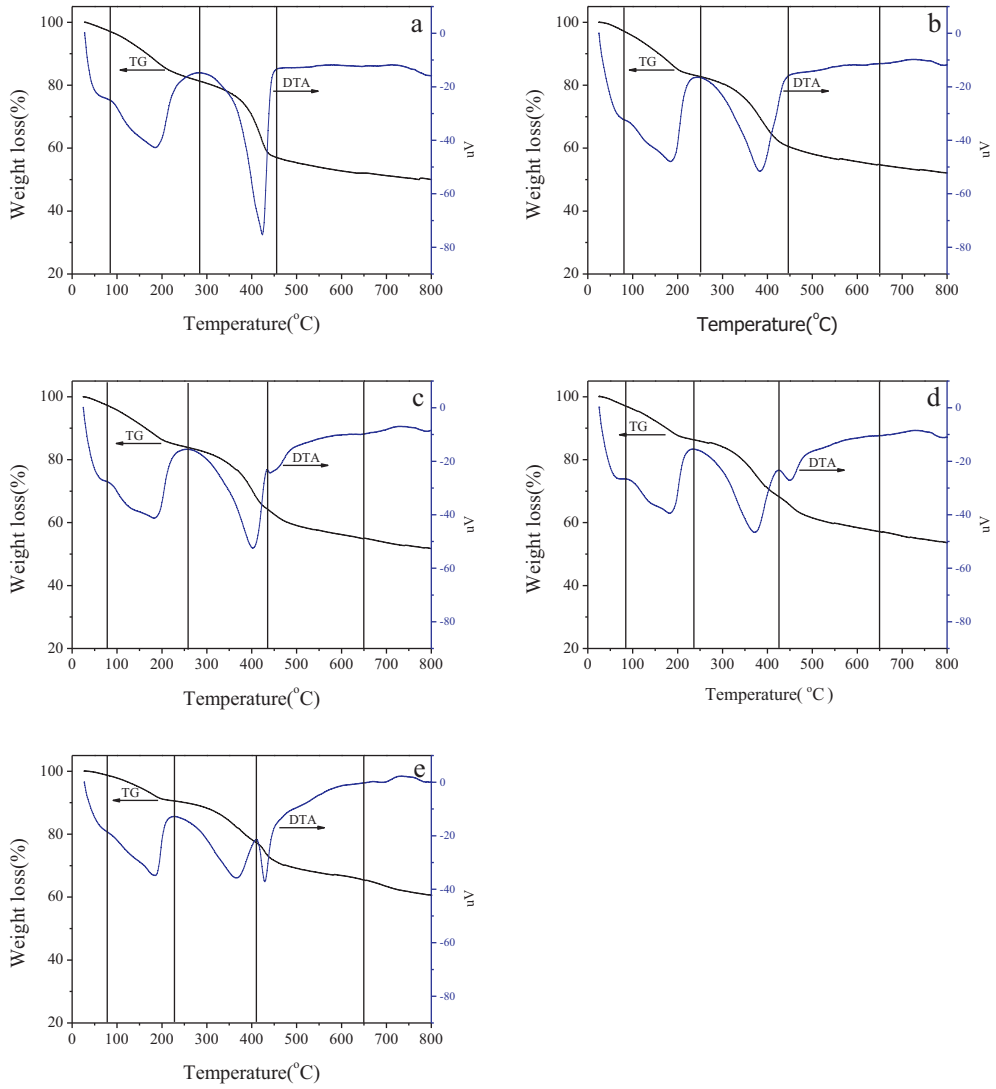

Fig. 1. TG-DTA curves of *x*La-HTLcs samples (a) $x = 0$, (b) $x = 0.1$, (c) $x = 0.4$, (d) $x = 0.7$, (e) $x = 1.0$.

features of H3 type (IUPAC classification). Type H3 hysteresis is usually associated with solids consisting of platy shaped particles. This is in accordance with the traditional view of these types of mixed oxides. Meanwhile, the hysteresis loops become narrow with the La content increase. This indicates that the pore becomes regular. The pore size distribution curve of the catalysts is gradually broadened as the La additive amount is increased.

Table 1 shows the nitrogen adsorption measurement data of the composite oxide catalysts *x*LHTs. It can be seen that the BET surface area increases from 77.4 to 115.1 $m^2\,g^{-1}$ and the pore volume increases from 0.29 to 0.73 $cm^3\,g^{-1}$ with the La content increasing from $x = 0$ to $x = 0.7$. The BET surface area and the pore volume are dramatically decreased when the x reaches 1.0, because of formation of new La_2O_3 structure. Along with the increased La additive amount, the BET surface area and pore volume reach 115.1 $m^2\,g^{-1}$ and 0.734 $cm^3\,g^{-1}$, respectively, when $x = 0.7$. However, when x reached 1.0, the surface area of *x*LHTs drops to 31.4 $m^2\,g^{-1}$.

Table 1
Specific surface area and pore parameter of *x*LHTs catalysts.

Catalysts	Surface area ($m^2\,g^{-1}$)	Pore volume[a]	Average pore size[a] (nm)
0LHTs	77.4	0.29	14.3
0.1LHTs	101.5	0.46	16.0
0.4LHTs	105.5	0.61	20.5
0.7LHTs	115.1	0.73	24.1
1.0LHTs	31.4	0.20	25.0

[a] Calculated based on adsorption branch of isotherm.

3.1.3. XRD analysis

The XRD patterns of all La-HTLcs samples are showed in Fig. 3. Apart from 1.0 La-HTLcs, all the samples exhibited similar profiles to the pure hydrotalcite, performing six feature diffraction peaks of (0 0 3), (0 0 6), (0 1 2) (0 1 5), (0 1 8), (1 1 0) and (1 1 3), which indicate the crystalline formation of layered double hydroxide structure of HT [30,31]. Peaks intensities and sharpness of (0 0 3) and (0 0 6) planes, which are directly proportional to the crystallinity of material, were observed to decrease on increasing the La content of hydrotalcite. And its crystallinity decreases with the La content addition. Finally, such HTLcs structure disappeared when the La additive amount reached $x = 1.0$.

The XRD patterns of the *x*LHTs are presented in Fig. 4. It can be observed that the layered crystalline structure of HTLcs is destroyed during calcination. For *x*LHTs of $x = 0$, 0.1, 0.4 and 0.7, the structure of samples changes from orthorhombic to cubic, corresponding to the transformation of a two-dimensional layered structure to a three-dimensional structure and it is converted into a type of Mg–Al

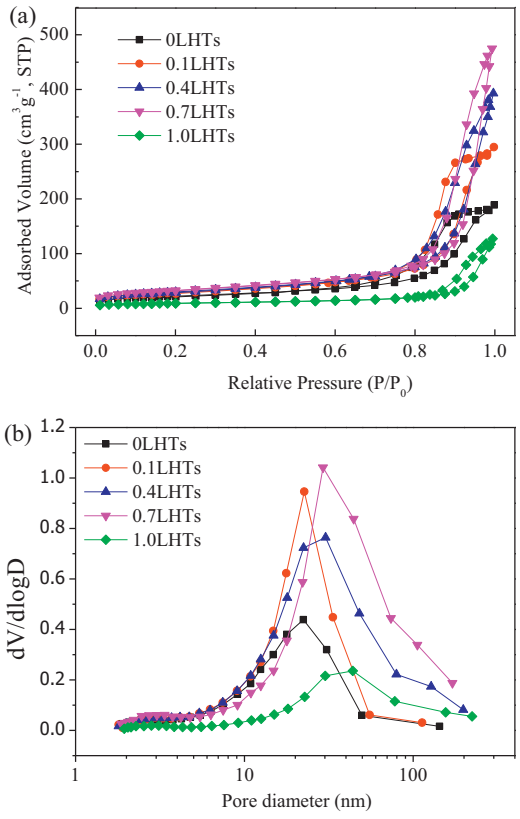

Fig. 2. N_2 adsorption–desorption isotherms (a) and pore distribution (b) of *x*LHTs catalysts.

composite oxide. As the La additive amount increased to $x = 1.0$, the XRD spectrum displayed the phase of La oxide only.

3.1.4. FT-IR analysis

FT-IR spectra for the samples of *x*La-HTLcs are shown in the Fig. 5. All the samples show rather similar spectra. The broad band is recorded around 3450–3500 cm^{-1} due to the stretching vibrations of structural hydroxyl groups, which exist in the HTLcs layers and the water molecules in the interlays space [32,33]. A rather weak band at 1640 cm^{-1} is attributed to the deformation vibrations of interlayer water molecules [31]. The bands around 1350–1390 cm^{-1} is ascribed to the v_3 mode of interlayer carbonate species. For the samples 0La-HTLcs, 0.1La-HTLcs, 0.4La-HTLcs and 0.7La-HTLcs, it is found that this single vibration splits into

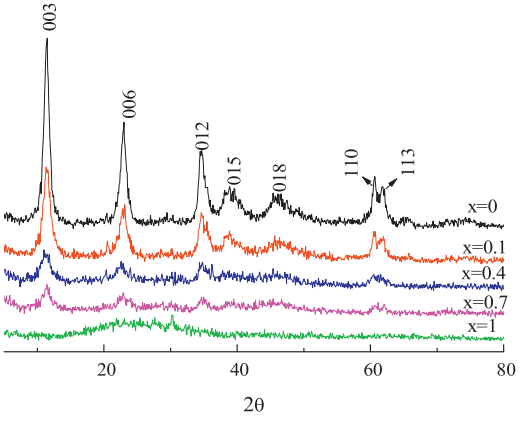

Fig. 3. XRD patterns of *x*La-HTLcs.

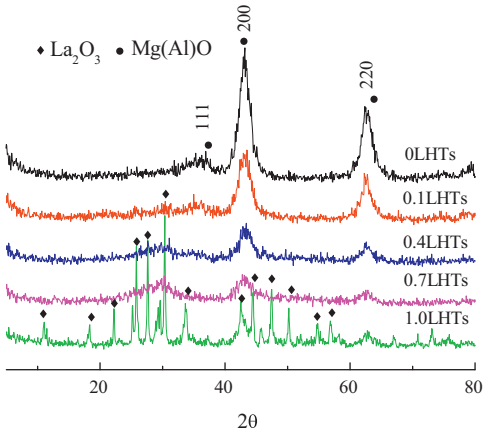

Fig. 4. XRD patterns of *x*LHTs calcined at 650 °C.

two bands because of lowering in the local symmetry of the carbonate anion in the interlayer space [34]; the extremely weak band at 1060 cm^{-1} is attributed to the v_1 mode of carbonate species. The bands observed at 856 cm^{-1}, 680 cm^{-1} and 443 cm^{-1} are due to the Mg—OH stretching and Mg—OH—M (Al, La) bending vibration [27].

3.1.5. CO_2-TPD analysis

The surface basicity of composite oxides catalysts was measured by CO_2-TPD and the basic species could be assigned according to the temperature at which peaks appeared. The CO_2-TPD curves are shown in Fig. 6. The basic species was studied by means of CO_2-TPD peak-differentiation-imitating analysis. All the profiles can be split into three Gaussian peaks. As reported by León, the formation of different species stems from the presence of sites with difference basic strength in the CO_2 adsorption and desorption process: bicarbonates (OH, weak base sites), bidentate carbonates (bridging and chelating, M^{m+}–O^{2-} pairs, medium-strength base sites) or unidentates (O^{2-}, strong base sites). Associating these types of species with the CO_2 desorption temperature, it is clear that weak base sites correspond to the range 20–100 °C, bridging bidentate carbonate with 100–200 °C, chelating bidentate carbonate with 200–300 °C and unidentate carbonate with temperatures over 300 °C [35]. According to information above, it is clarified that all the three peaks be assigned to weak basic sites, moderate basic sites and strong basic sites, respectively. However, the moderate basic sites of 1.0LHTs belong to bridging bidentate carbonate, while the moderate basic sites of other catalysts belongs to chelating bidentate carbonate.

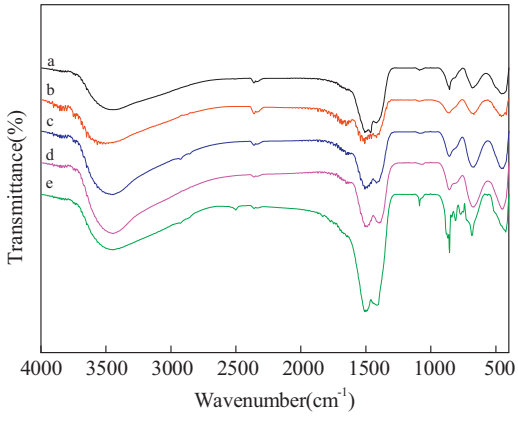

Fig. 5. FT-IR spectra of *x*La-HTLcs samples (a) $x = 0$, (b) $x = 0.1$, (c) $x = 0.4$, (d) $x = 0.7$, (e) $x = 1.0$.

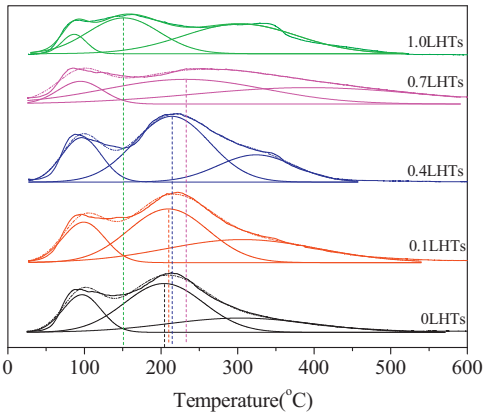

Fig. 6. Temperature-programmed desorption using CO_2.

It can be clearly observed that the moderate basic strength is enhanced with the La content increasing and it reaches the highest desorption temperature when the *x* is 0.7. But when the La content *x* is as high as 1.0, the chelating bidentate carbonate sites disappear and the moderate basic sites are replaced by bridging bidentate carbonate sites.

3.1.6. SEM analysis

SEM was applied to study the morphological properties of the as-synthesized catalysts. SEM images of catalysts calcined at 650 °C are compared in Fig. 7. It can be observed that the catalyst of (a) 0LHTs, (b) 0.1LHTs, (c) 0.4LHTs and (d) 0.7LHTs exhibits a layered and platelet-like structure, while the structure of (e) 1.0LHTs is different. For the 0LHTs catalyst, it is clear that its surface of platelet is smooth, which is the same as reported in Refs. [36,37]. However, the platelet surface becomes rough and fluffy along with the La content increasing and it no longer has the platelet structure when La content is as high as 1.0. This result is well in accordance with the result of XRD analysis.

3.2. Catalytic performance

3.2.1. The effects of La content

The catalytic performance of *x*LHTs for the DPC synthesis is compared in Table 2. It is apparent that the as-prepared composite oxide catalysts derived from different HTLcs precursors exhibit different catalytic performance in the transesterification reaction.

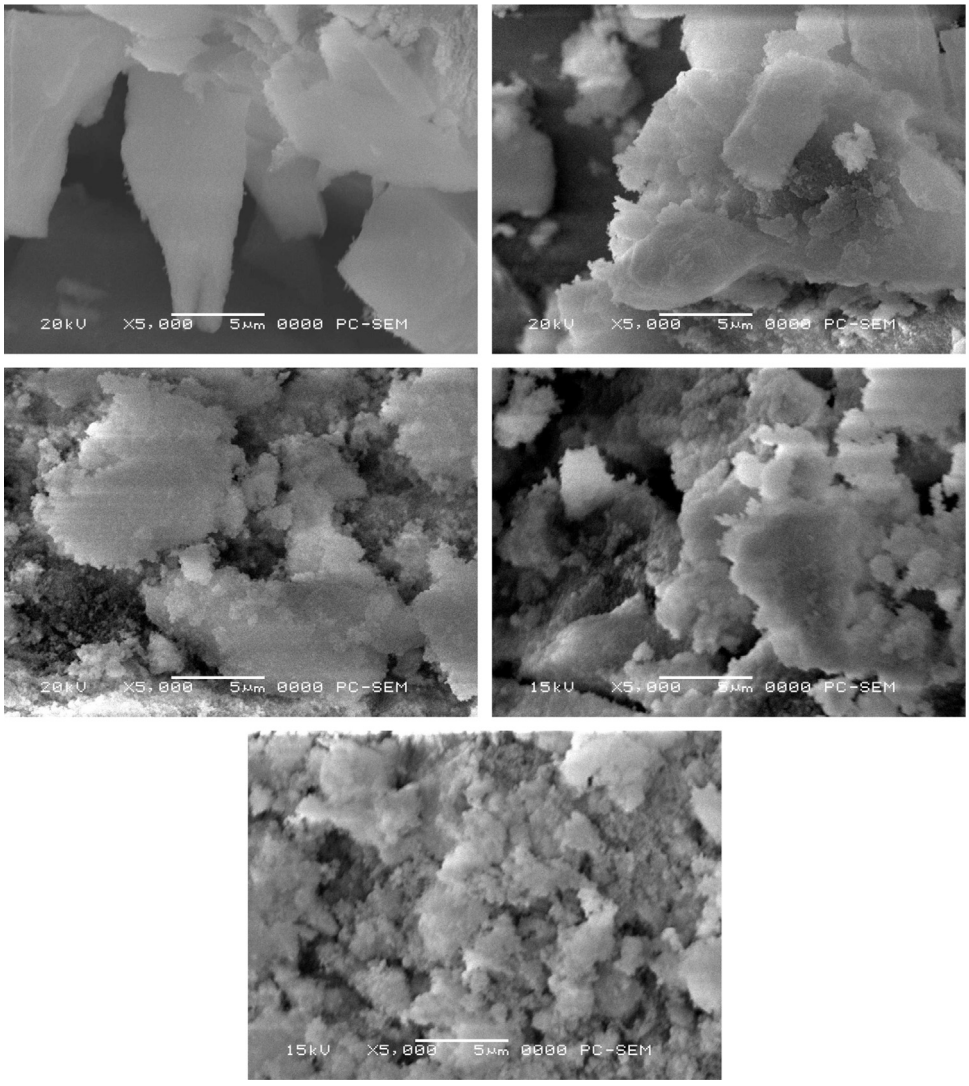

Fig. 7. SEM images of the catalysts: (a) 0LHTs, (b) 0.1LHTs, (c) 0.4LHTs (d) 0.7LHTs (e) 1.0LHTs.

Table 2
Activities of *x*LHTs for the DPC synthesis.

Catalysts	DMC conv. (%)	DPC sel. (%)	DPC yield (%)
0LHTs	98.2	71.3	70.0
0.1LHTs	98.1	72.7	71.3
0.4LHTs	99.2	93.6	92.9
0.7LHTs	98.4	95.4	93.9
1.0LHTs	98.0	85.1	83.4

(Reaction conditions: *n*(n-propanol):*n*(DMC) = 3:1; *m*(catalyst):*m*(reactant) = 0.03; 90 °C;6 h)

Under identical reaction conditions, the Al–Mg composite oxide catalyst from the HTLcs precursor without La addition indicates that the DMC conversion and the DPC selectivity are 98.2% and 71.3%, respectively. The by-product is methyl propyl carbonate (MPC). With the La content increasing, the selectivity of DPC increases. And when *x* is 0.7, the DPC selectivity reaches a maximum of 95.4%. However, when the La content further reaches 1.0, the selectivity of DPC turns to decrease. Generally, the catalytic performance of the catalysts is not only related to their catalytic base sites, but also correlated with their structure. It was reported that the calcined Al–Mg hydrotalcite showed the catalytic activity of alkylation via the base active sites [24]. The current activity tests suggest that La additive in the Al–Mg composite oxides from HTLcs precursor can remarkably improve the product selectivity toward DPC synthesis via the transesterification of DMC and propanol. And this enhancement is owing to the adjustment of the base sites properties by La additive.

3.2.2. The effect of the reaction time

Fig. 8 shows the effect of reaction time on DPC production. It is indicated that the conversion of DMC and the selectivity of DPC increase gradually with the reaction time increasing within the first 6 h. Meanwhile, the selectivity of MPC reaches 96.4% after 1 h, but decreases rapidly with the reaction proceeding, suggesting that MPC is the intermediate product in this reaction.

3.2.3. The effect of the catalyst dosage

The effect of 0.7LHTs dosage on the catalytic performance is presented in Fig. 9. It is indicated that the DMC conversion does not obviously change with the increased catalyst dosage. When the dosage is kept above 2.0%, the catalysts sustain high and stable performance.

3.2.4. The reusability of the catalyst

The reusability of the catalyst was also tested over 0.7LHTs. The catalyst was continuously tested for six times and the results are displayed in Fig. 10. After each reaction the catalyst was filtered, dried and then reused. It is clear that both the DMC conversion and the DPC selectivity are almost unchanged. These findings indicate that the catalysts have good reusability toward the DPC synthesis via the transesterification between DMC and propanol.

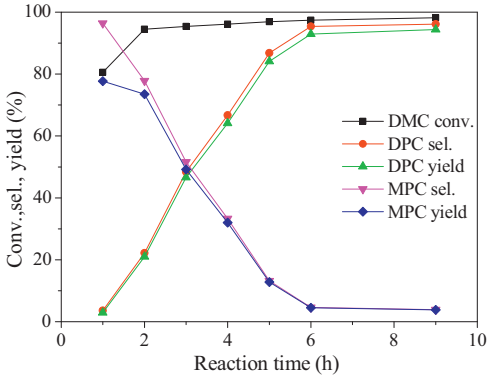

Fig. 8. Effect of reaction time.

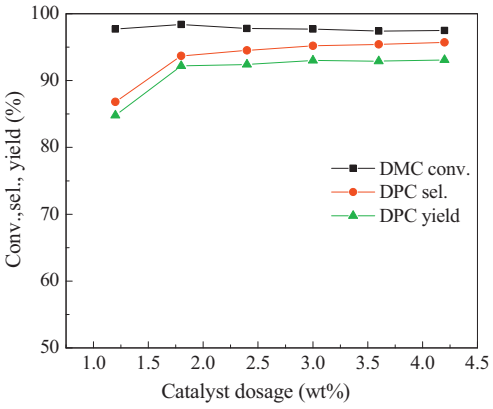

Fig. 9. Effect of the catalyst dosage on the activity.

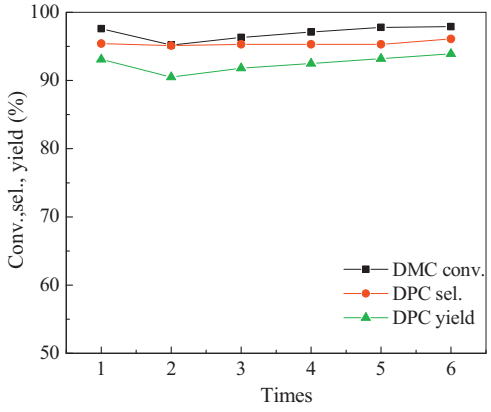

Fig. 10. Reuse tests of 0.7LHTs.

4. Conclusions

The Mg–Al and La–Mg–Al composite oxide catalysts were prepared via calcining the precursors of hydrotalcite-like compounds (HTLcs) from co-precipitation method and they exhibited high catalytic activities for the DPC synthesis via transesterification of DMC and propanol. When the HTLcs precursor with a La:Mg:Al molar ratio of 0.7:3:1 was calcined at 650 °C, the obtained catalyst displayed the best catalytic activity. Under the stipulated reaction conditions, the maximum conversion of DMC and selectivity of DPC reached above 98% and 95.4%, respectively.

The catalyst characterization results suggested that the La content played an important role in tuning the structural and morphological properties of the catalysts. The platelet surface became rough and fluffy along with the La content increasing and it no longer had the platelet structure when La content reached 1.0. It was also found that the moderate strength basic sites enhanced with the La content increasing and it reached to the highest desorption temperature when the *x* rose to 0.7. As the La content *x* increased to 1.0, the chelating bidentate carbonate sites disappeared and the moderate basic sites were replaced by bridging bidentate carbonate sites. The moderate strength basic sites were the catalytic centers in this reaction.

Acknowledgements

The authors thank for the financial support of Major Project of Chinese National Programs for Fundamental R & D (2012CB723106) and International Cooperation Project from Chinese Ministry of Science and Technology (2010DFB40440).

Appendix A. Supplementary data

Supplementary data associated with this article can be found, in the online version, at http://dx.doi.org/10.1016/j.apcata.2013.05.026.

References

[1] A.-A.G. Shaikh, S. Sivaram, Chem. Rev. 96 (1996) 951–976.
[2] P. Tundo, M. Selva, Acc. Chem. Res. 35 (2002) 706–716.
[3] D. Delledonne, F. Rivetti, U. Romano, Appl. Catal. A: Gen. 221 (2001) 241–251.
[4] M.A. Pacheo, C.L. Marshall, Energy Fuels 11 (1997) 2–29.
[5] Y.T. Kim, E.D. Park, Appl. Catal. A: Gen. 361 (2009) 26–31.
[6] Y.T. Kim, E.D. Park, Appl. Catal. A: Gen. 356 (2009) 211–215.
[7] W. Zhou, X. Zhao, Y. Wang, J. Zhang, Appl. Catal. A: Gen. 260 (2004) 19–24.
[8] G. Zhao, J. Shi, G. Liu, Y. Liu, Z. Wang, W. Zhang, M. Jia, J. Mol. Catal. A: Chem. 327 (2010) 32–37.
[9] T. Keller, J. Holtbruegge, A. Górak, Chem. Eng. J. 180 (2012) 309–322.
[10] S.M. Gade, M.K. Munshi, B.M. Chherawalla, V.H. Rane, A.A. Kelkar, Catal. Commun. 27 (2012) 184–188.
[11] F.S.H. Simanjuntak, T.K. Kim, S.D. Lee, B.S. Ahn, H.S. Kim, H. Lee, Appl. Catal. A: Gen. 401 (2011) 220–225.
[12] M. Tudorache, L. Protesescu, A. Negoi, V.I. Parvulescu, Appl. Catal. A: Gen. 437–438 (2012) 90–95.
[13] Y.H. Taufiq-Yap, H.V. Lee, R. Yunus, J.C. Juan, Chem. Eng. J. 178 (2011) 342–347.
[14] T. Chen, H. Han, J. Yao, G. Wang, Catal. Commun. 8 (2007) 1361–1365.
[15] X. He, Z. Li, K. Su, B. Cheng, J. Ming, Catal. Commun. 33 (2013) 20–23.
[16] H. Niu, J. Yao, Y. Wang, G. Wang, J. Mol. Catal. A: Chem. 235 (2005) 240–243.
[17] Y. Li, Y. Zhang, B. Xue, Y. Guo, J. Mol. Catal. A: Chem. 287 (2008) 9–15.
[18] X. Chen, Y. Dong, C. Zhao, T. Zhao, Energy Fuels 22 (2008) 3571–3574.
[19] M.R. Pérez, I. Crespo, M.A. Ulibarri, C. Barriga, V. Rives, J.M. Fernández, Mater. Chem. Phys. 132 (2012) 375–386.
[20] S.H. Wang, Y.B. Wang, Y.M. Dai, J.M. Jehng, Appl. Catal. A: Gen. 439–440 (2012) 135–141.
[21] D. Tichit, D. Lutic, B. Coq, R. Durand, R. Teissier, J. Catal. 219 (2003) 167–175.
[22] L. Faba, E. Díaz, S. Ordóñez, Appl. Catal. B: Environ. 113–114 (2012) 201–211.
[23] M. Mokhtar, T.S. Saleh, S.N. Basahel, J. Mol. Catal. A: Chem. 353–354 (2012) 122–131.
[24] Y. Liu, E. Lotero, J.G. Goodwin, X. Mo, Appl. Catal. A: Gen. 331 (2007) 138–148.
[25] M.G. Alvarez, A.M. Segarra, S. Contreras, J.E. Sueiras, F. Medina, F. Figueras, Chem. Eng. J. 161 (2010) 240–345.
[26] D.A. Aguilera, A. Perez, R. Monlina, S. Moreno, Appl. Catal. B: Environ. 104 (2011) 144–150.
[27] W. Yang, Y. Kim, P.K.T. Liu, M. Sahimi, T.T. Tsotsis, Chem. Eng. Sci. 57 (2002) 2945–2953.
[28] J.P. Ramirez, J. Overeijnder, F. Kapteijn, J.A. Moulijn, Appl. Catal. B: Environ. 23 (1999) 59–72.
[29] E.M. Seftel, M. Mertens, P. Cool, Appl. Catal. B: Environ. 134-135 (2013) 274–285.
[30] A. Schutz, P. Biloen, J. Solid State Chem. 68 (1987) 360–368.
[31] S. Kannan, A. Dubey, H. Knozinger, J. Catal. 231 (2005) 381–392.
[32] D. Wan, H. Liu, R. Liu, J. Qu, S. Li, J. Zhang, Chem. Eng. J. 195–196 (2012) 241–247.
[33] J.A. Rivera, G. Fetter, Y. Jiménez, M.M. Xochipa, P. Bosch, Appl. Catal. 316 (2007) 207–211.
[34] M. Crivello, C. Pe'rez, J. Ferna'ndez, G. Eimer, E. Herrero, S. Casuscelli, E.R. Castello'n, Appl. Catal. A: Gen. 317 (2007) 11–19.
[35] M. León, E. Díaz, S. Bennici, A. Vega, S. Ordóñez, A. Auroux, Ind. Eng. Chem. Res. 49 (2010) 3663–3671.
[36] K. Takehira, T. Shishido, D. Shouro, K. Murakami, M. Honda, T. Kawabata, K. Takaki, Appl. Catal. A: Gen. 279 (2005) 41–51.
[37] C.E. Daza, C.R. Cabrera, S. Moreno, R. Molina, Appl. Catal. A: Gen. 378 (2010) 125–133.